ON-LINE APPENDIX

On-line Method 1: Multiatlas ROI Segmentation

Multiatlas segmentation has engendered increasing interest in recent years and has shown clear improvement in accuracy over single-atlas-based segmentation.[1] In this framework, semi-automatically extracted reference ROI labels from multiple atlases are warped individually to the target image and are fused together to assign a label to each voxel of the target images. The proposed method[2] uses a consensus labeling framework, by generating a broad ensemble of labeled atlases via the use of 2 different nonlinear image registration algorithms, followed by a spatially adaptive weighted voting strategy to fuse the ensemble into a final segmentation. The brain was segmented into a set of 154 anatomic ROIs, which were organized within a hierarchic structure to allow derivation of volumetric measurements in various resolution levels. The method includes nonlinear registration of multiple atlases with ground-truth labels for every individual scan,[3] followed by a local similarity-based fusion of labels from different atlases.

In the fusion, a local similarity term is used for ranking and weighting reference labels from different atlases, and an image-intensity-based term is used for modulating the segmentations in the boundaries of the ROIs according to the intensity profile of the subject image. On-line Fig 2 shows sample segmentation.

On-line Method 2: Pattern Classification

The SPARE-AD index is derived from a support vector machine classifier (for more mathematical formulation, see Vapnik[4] and Habes et al[5]) trained for optimal discrimination between healthy controls and age-matched patients with AD[6,7] and summarizes the high-dimensional image data with a single score that indicates the distance of the test sample from the classification hyperplane. As input, we used regional volumetric maps called Regional Analysis of Volumes Examined in Normalized Space,[7-9] which were obtained by using tissue-preserving image warping, to enable comparative analysis of tissue volumes in the common template space. In this study, we used gray matter Regional Analysis of Volumes Examined in Normalized Space maps that were normalized by intracranial volume to adjust for global differences in head size.

More positive SPARE-AD implies a more Alzheimer disease-like brain structure, and more negative SPARE-AD implies more normal structures.[10] The SPARE-AD model was trained on the external training dataset described in Da et al[6] and was validated earlier.[8,9]

On the other hand, the SPARE-BA index captures aging-related brain structural changes and was developed earlier by using a training model from the SHIP study as described in Habes et al.[10,11] As validation of the SPARE-BA index within SHIP, we used 2 metrics: 1) the cross-validated classification accuracy of the model for the training dataset (area under curve = 0.96), showing that the model can successfully detect discriminative imaging patterns that separate old and young subjects; 2) the Spearman rank correlation between the actual age and the calculated SPARE-BA index of a subject ($r = -0.80$), showing that the model has predictive power for determining the brain age of a subject. We used the default value = 1 in the LIBSVM[12] implementation for the penalty misclassification parameter (denoted usually as C in the literature[4]) for both SPARE-AD and SPARE-BA models.

On-line Method 3: APOE *Determination in SHIP*

From SHIP-0, 4081 individuals were successfully genotyped by using the Genome-Wide Human SNP Array 6.0 (Affymetrix, Santa Clara, California). The total number of SNPs after imputation and quality control was 2,748,910. Genotyping of SHIP-TREND (986 individuals) was performed by using the HumanOmni2.5-Quad (Illumina, San Diego, California). The total number of SNPs after imputation and quality control was 3,437,411. Genotypes in SHIP-0 were determined by using the Birdseed2 clustering algorithm. Genotypes in SHIP-TREND were called with the GenCall algorithm of GenomeStudio Genotyping Module, Version 1.0 (Illumina). The genetic data analysis workflow was created by using the Software InforSense (http://inforsense.software.informer.com/download/).

The *APOE* genotypes were determined on the basis of rs429358(C;C) and rs7412(T;T) from the resulting imputation (overall imputation quality, >0.8; Hardy-Weinberg Equilibrium, $P > .05$). Because we used the genomewide association study dataset and not strand-specific genotyping for determination of *APOE* status, 2 ambiguous SNP combinations occurred when *APOE* $\varepsilon 2/\varepsilon 4$ and $\varepsilon 1/\varepsilon 3$ could not be discriminated (http://www.snpedia.com/index.php/*APOE*). To deal with this limitation, we first determined the effect of *APOE* $\varepsilon 4$ after leaving out the cases with the unidentifiable combination $\varepsilon 2/\varepsilon 4$ and $\varepsilon 1/\varepsilon 3$. In this study, all cases with $\varepsilon 2/\varepsilon 4$ or $\varepsilon 1/\varepsilon 3$ were excluded ($n = 35$).

REFERENCES

1. Iglesias JE, Sabuncu MR. **Multi-atlas segmentation of biomedical images: a survey.** *Med Image Anal* 2015;24:205–19 CrossRef Medline
2. Doshi J, Erus G, Ou Y et al; Alzheimer's Neuroimaging Initiative. **MUSE: MUlti-atlas region segmentation utilizing ensembles of registration algorithms and parameters, and locally optimal atlas selection.** *Neuroimage* 2016;127:186–95 CrossRef Medline
3. Ou Y, Sotiras A, Paragios N et al **DRAMMS: deformable registration via attribute matching and mutual-saliency weighting.** *Med Image Anal* 2011;15:622–39 CrossRef Medline
4. Vapnik VN. *The Nature of Statistical Learning Theory*. New York: Springer-Verlag; 2000
5. Habes M, Schiller T, Rosenberg C et al. **Automated prostate segmentation in whole-body MRI scans for epidemiological studies.** *Phys Med Biol* 2013;58:5899–915 CrossRef Medline
6. Da X, Toledo JB, Zee J et al **Integration and relative value of biomarkers for prediction of MCI to AD progression: spatial patterns of brain atrophy, cognitive scores, APOE genotype and CSF biomarkers.** *Neuroimage Clin* 2014;4:164–73 CrossRef Medline
7. Davatzikos C, Xu F, An Y et al. **Longitudinal progression of Alzheimer's-like patterns of atrophy in normal older adults: the SPARE-AD index.** *Brain* 2009;132:2026–35 CrossRef Medline
8. Fan Y, Shen D, Gur RC et al. **COMPARE: Classification of Morphological Patterns Using Adaptive Regional Elements.** *Med Imaging IEEE Trans* 2007;26:93–105 CrossRef Medline
9. Fan Y, Batmanghelich N, Clark CM et al; Alzheimer's Disease Neuroimaging Initiative. **Spatial patterns of brain atrophy in MCI**

patients, identified via high-dimensional pattern classification, predict subsequent cognitive decline. *Neuroimage* 2008;39:1731–43 Medline

10. Habes M, Erus G, Toledo JB, et al. **White matter hyperintensities and imaging patterns of brain ageing in the general population.** *Brain* 2016;139(pt 4):1164–79 CrossRef Medline
11. Habes M, Janowitz D, Erus G, et al. **Advanced brain aging: relationship with epidemiologic and genetic risk factors, and overlap with Alzheimer disease atrophy patterns.** *Transl Psychiatry* 2016;6:e775 CrossRef Medline
12. Chang CC, Lin CJ. **LIBSVM: a library for support vector machines.** https://www.csie.ntu.edu.tw/~cjlin/libsvm/. Accessed July 2014

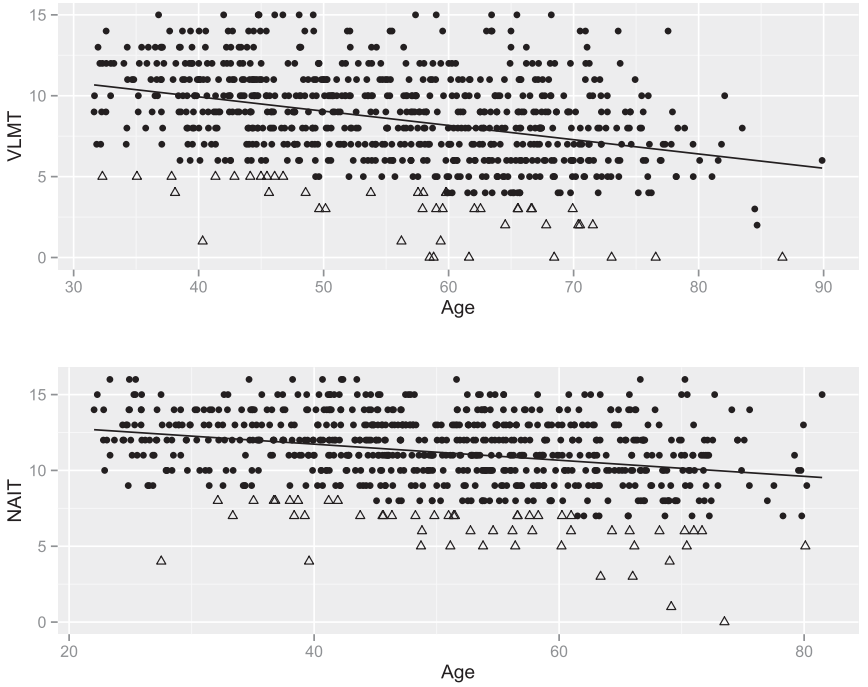

ON-LINE FIG 1. Cognitively impaired subjects (*triangles*, $n = 98$) in SHIP-2/SHIP-TREND categorized on the basis of their cognitive score (Verbal Learning and Memory Test for the subcohort SHIP-2 [$n = 744$], and the Nuremberg Age Inventory Test for the subcohort SHIP-TREND [$n = 728$]) depicted by age. *Circles* represent cognitively healthy individuals.

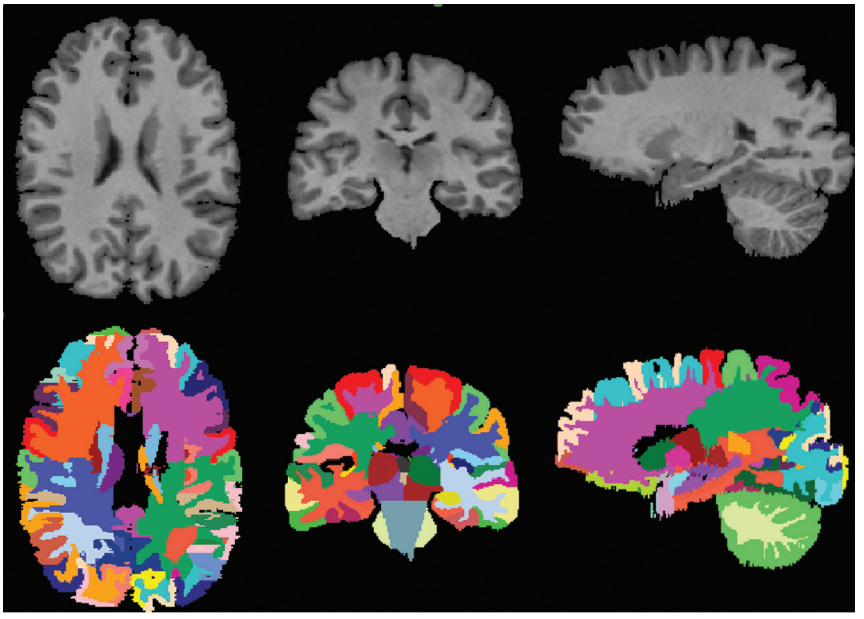

ON-LINE FIG 2. Segmentation into anatomic ROIs.

On-line Table 1: Description of the SHIP participants with MRI data excluded in this study[a] because of missing data[b]

Characteristic	SHIP-2 Excluded	SHIP-TREND Excluded	SHIP-2+TREND Excluded
Age (median) (SD) (yr)	57.53 (13.83)	52.56 (14.40)	53.77 (14.47)
Education (No.) (%)			
<8 yr	96 (28.15)	224 (17.77)	320 (19.98)
8–10 yr	168 (49.26)	671 (53.25)	839 (52.40)
>10 yr	77 (22.58)	365 (28.96)	442 (27.60)
Female sex (No.) (%)	165 (48.38)	610 (48.41)	775 (48.40)[c]
Verbal Learning and Memory Test (mean) (SD)	8.70 (2.49)		
Nuremberg Age Inventory (mean) (SD)		11.24 (2.56)	

[a] Values are for the corresponding available demographic data.
[b] No significant difference was detected between the sample excluded compared with the sample included in this study except for sex.
[c] Significant difference compared with the sample included in this study.

On-line Table 2: Linear regression models between age and ROI volumes (normalized by total intracranial volume) and SPARE-AD and SPARE-BA for subjects in the age range of 22–40 years ($n = 248$)[a]

Outcome	Age	Sex	*APOE ϵ4* Carriers
Lateral frontal volume	−0.0004465 (<.001)[b]	0.0018230 (.004)[b]	−0.0006391 (.356)
Lateral temporal volume	−0.0000946 (.027)[b]	0.0008911 (.019)[b]	0.0004538 (.283)
Medial frontal volume	−0.0001090 (<.001)[b]	0.0008957 (<.001)[b]	0.0001964 (.428)
Hippocampal volume	0.0000048 (.370)	0.0001269 (.008)[b]	0.0000479 (.371)
SPARE-AD	0.0132300 (.230)	−0.2535700 (.010)[b]	−0.0605400 (.580)
SPARE-BA	−0.1033300 (<.001)[b]	0.5936500 (<.001)[b]	−0.1082300 (.439)

[a] Data are coefficient (*P* value).
[b] Significant at $P < .05$. Models are adjusted for education and study cohort effects.

On-line Table 3: Linear regression models between age and ROI volumes (normalized by total intracranial volume) and SPARE-AD and SPARE-BA for subjects older than 60 years of age ($n = 487$)[a]

Outcome	Age	Sex	*APOE ϵ4* Carriers
Lateral frontal volume	−0.0004076 (<.001)[b]	0.0028070 (<.001)[b]	0.0001572 (.772)
Lateral temporal volume	−0.0002414 (<.001)[b]	0.0006251 (.063)	0.0002931 (.461)
Medial frontal volume	−0.0001480 (<.001)[b]	0.0013340 (<.001)[b]	0.0000497 (.825)
Hippocampal volume	−0.0000341 (<.001)[b]	0.0001983 (<.001)[b]	−0.0000075 (.872)
SPARE-AD	0.0689980 (<.001)[b]	−0.2136610 (.009)[b]	0.0227590 (.814)
SPARE-BA	−0.1094700 (<.001)[b]	0.7808200 (<.001)[b]	0.0446400 (.728)

[a] Date are coefficient (*P* value).
[b] Significant at $P < .05$. Models are adjusted for education and study cohort effects.

On-line Table 4: Linear regression model with age, sex, education level, and *APOE* status as independent variables and VLMT as a dependent variable

	VLMT SHIP-2 Participants ($n = 744$)		
Factor	Estimate	SE	*P* Value (Factor)
Age (yr)	−0.086	0.009	<.001[a]
Female sex	1.114	0.199	<.001[a]
Education			
8–10 yr	−0.087	0.292	.766
>10 yr	1.075	0.323	.001[a]
APOE status, at least 1 *ϵ4* allele	0.254	0.250	.311
	$R^2 = 0.187$		

Note:—SE indicates standard error; VLMT, Verbal Learning and Memory Test.
[a] Significant at $P < .05$.

On-line Table 5: Linear regression model with age, sex, education level, and *APOE* status as independent variables and NAI as a dependent variable

	NAI SHIP-TREND Participants ($n = 728$)		
Factor	Estimate	SE	*P* Value (Factor)
Age (yr)	−0.046	0.007	<.001a
Female sex	1.064	0.174	<.001[a]
Education			
8–10 Years	1.064	0.301	<.001[a]
>10 Years	1.745	0.315	<.001[a]
APOE status, at least 1 ϵ4 allele	0.020	0.200	.919
	$R^2 = 0.156$		

Note:—NAI indicates Nuremberg Age Inventory; SE, standard error.
[a] Significant at $P < .05$.